Transactions of the **14th International Conference on Structural Mechanics in Reactor Technology** (SMiRT 14), Lyon, France, August 17-22, 1997 **K13/5**

Analytical study of frequency effects on seismic margins

Huang C.T.[(1)], **Iwan W.D.**[(1)], **Jaquay K.R.**[(2)], **Chokshi N.C.**[(3)]
(1) California Institute of Technology, USA
(2) Boeing North American, Inc., USA
(3) U.S. Nuclear Regulatory Commission, USA

ABSTRACT: This paper presents an ongoing analytical study of frequency effects on seismic fatigue margins of nuclear power plant piping. The study focuses on simulated seismic testing of piping components conducted as part of the previous joint EPRI/NRC PFDR program. The paper describes the techniques developed for modeling and identification of hysteresis loops exhibited during PFDR tests, two approaches for the analytical extrapolation of these tests for frequency ratios not tested, and the identification of a large deformation failure mode not being addressed by the seismic fatigue margin.

1 INTRODUCTION

The 1994 Addenda to the ASME Boiler and Pressure Vessel Code, Section III, increases the allowable primary stress limit for the Service Level D Safe Shutdown Earthquake in the design of nuclear power plant piping. The increase was based primarily on seismic fatigue margin studies of simulated seismic tests of 33 piping components conducted during the Electric Power Research Institute (EPRI) / U.S. Nuclear Regulatory Commission (NRC) Piping and Fitting Dynamic Reliability (PFDR) Program. The seismic fatigue margin was taken to be the ratio of the peak acceleration that would have been required to cause a through-wall crack in the component at the end of one application of a given loading time history to the peak acceleration of the same loading time history when scaled down to the level that the allowable primary stress limits are just met in a Code analysis. The simulated seismic tests were conducted using a narrow-banded input excitation tuned to have a peak frequency near the natural frequency of the test components. These tests indicated that the minimum seismic fatigue margin using the new Code design rules was 4.2. Based on the tests, it was also concluded that fatigue failure was the only failure mode that needed to be considered in the seismic design of nuclear power plant piping.

Since the natural frequencies of piping systems in nuclear power plants may vary over a fairly wide range, an attempt was made to extend the limited frequency range of the PFDR test results by analytical means. These attempts indicated that the seismic fatigue margins generally decreased away from a resonance condition but remained above acceptable levels over a wide range of piping frequencies. As a result of further study using unbroadened spectra in the Code analysis and including pressure stresses, the minimum seismic fatigue margin was reduced to 2.1, still supporting rule developer arguments that piping systems in nuclear power plants can be safely designed to the new higher stress limits.

However, NRC staff members on the Code rule committees and a subsequent NRC-funded independent evaluation of the PFDR seismic margins at the Energy Technology Engineering Center (ETEC), raised issues regarding the validity of the seismic fatigue margin studies.

Issues were also raised on the possibility of ratcheting collapse failure modes in addition to fatigue failures. In an effort to address some of these issues, the authors have performed a new analytical study of seismic fatigue margins using state-of-the-art nonlinear hysteretic system modeling and parameter optimization techniques.

2 FORMULATION OF COMPONENT TEST SYSTEMS

A generalized test configuration for the typical piping component test systems used in the PFDR program is shown in Fig. 1. To simplify the dynamic analyses for such systems, the dynamic response above a certain location on the piping component is assumed to be rigid body motion. The restoring moment developed in the piping component is then modeled as a nonlinear rotational spring. This results in a simple single-degree-of-freedom (SDOF) idealized analytical model as illustrated in Fig. 2. It is further assumed that the displacement response is "small" which allows the exclusion of the dynamic effects due to parametric excitation and geometrical nonlinearity. Based on these assumptions, the equation of motion governing the rotational angle response θ can be derived as

$$m\ddot{\theta} + k_{p\delta}\theta + f_r(\theta,\dot{\theta}) = c_f a(t) + f_e \tag{1}$$

where m, $k_{p\delta}$, c_f, f_e, $f_r(\theta,\dot{\theta})$, and $a(t)$ are respectively the generalized mass moment of inertia, P-Δ stiffness, excitation participation factor, sustained eccentric moment, the restoring moment of the piping component, and the measured sled acceleration time history.

Eqn. (1) stipulates the dynamic balance associated with the restoring moment and can be used to calculate the restoring moment characteristics using physical parameters and measured test data. Eqn. (1) also serves as the fundamental equation for the subsequent margin studies.

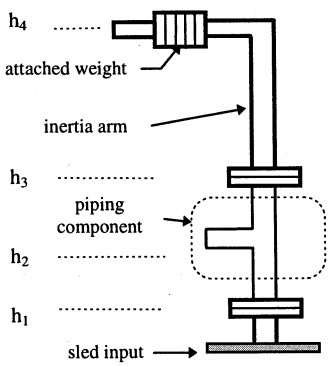

Figure 1: Typical test configuration of piping component test systems (Test 36)

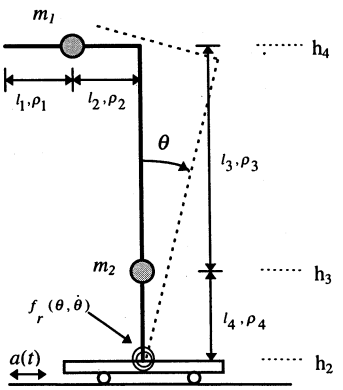

Figure 2: Idealized SDOF analytical model

3 MODELING AND IDENTIFICATION OF RESTORING MOMENT

The restoring moment $f_r(\theta,\dot{\theta})$ is assumed to consist of linear and hysteretic components given by

$$f_r(\theta,\dot{\theta}) = c\dot{\theta} + k_l\theta + h(\theta,\dot{\theta}) \tag{2}$$

where c, k_l and $h(\theta,\dot{\theta})$ are respectively the linear viscous damping, linear stiffness, and nonlinear hysteresis term. The hysteretic model considered is a class of hysteretic models capable of representing a broad range of curved non-deteriorating hysteretic behavior. These models are of the continuous parallel-distributed-element type [1] whose transient hysteretic behavior is fully determined by the initial loading curve [2]. By specifying an initial stiffness k_{ini} and a yielding moment f_y, simple mathematical functions such as the arctangent or hyperbolic tangent can be adopted to model the initial loading curve.

A parameter identification procedure associated with this class of hysteretic models is developed to obtain an optimal parameter set defining the restoring moment. The optimality sought is that the model generated response is as "close" to the measured data as possible. This results in a four dimensional optimization problem as

$$\text{Min} \quad J = J(k_{ini}, k_l, f_y, c) \tag{3}$$

where J symbolizes the objective function to be minimized, which can be taken as the sum square error of the difference between model generated and measured response.

The solution to the optimization problem is performed numerically on a developed computer program PIPES (Parameter Identification using Parallel-distributed-Element Systems). PIPES involves an integration of successive function evaluations and an optimization search scheme in the space spanned by the model parameters. The restoring moment-rotation characteristics calculated from the test data using basic mechanics is used to guide the optimal search within a plausible parameter range.

4 FATIGUE ANALYSIS

Using the optimized model, a fatigue analysis is then performed for a given input loading, based on the assumption that the nominal strain, ε, is linearly proportional to the rotational angle, θ, according to the relation

$$\varepsilon = \beta\theta \tag{4}$$

where β is a constant. The factor β is test-calibrated for each piping component test system such that the fatigue cumulative usage factor (CUF) reaches unity at the time a through-wall fatigue failure occurs. Miner's Linear Hypothesis is employed in analyzing the transient strain damage accumulation. Calculations of CUF can be conducted according to any given range-pair selection methods in conjunction with a selected fatigue curve.

5 FREQUENCY EFFECTS ON SEISMIC FATIGUE MARGIN

The seismic fatigue margin M_r for any given earthquake excitation is defined as

$$M_r = \frac{a_f}{a_c} \tag{5}$$

where a_f is the peak acceleration of the linearly amplified earthquake excitation required to result in fatigue failure at the conclusion of the earthquake excitation. a_c is the peak acceleration of the linearly amplified earthquake excitation resulting in Code design procedure calculated maximum allowable stresses. The Code design procedure was modified to use an unbroadened response spectra. This Code design procedure modification reflects the latest ASME consensus reached on test based margin definition.

The study of frequency effects considers a frequency ratio R_w defined as the ratio of the predominant frequency of the input earthquake to the test system's fundamental frequency.

With the test-calibrated nonlinear dynamic model and fatigue model available, extrapolation of the test-demonstrated fatigue margins can then be performed for similar test systems having an R_w other than the frequency ratio tested. To analytically achieve a different R_w, the analytical model is subjected to variations of the physical test configuration, or variations of the frequency content of the input loading. However, the model's nonlinear restoring moment characteristics must be left unchanged to preserve the test calibration. The sustained eccentric moment is excluded in the following consideration for simplicity. Both variations were employed in the frequency effects study and are described separately as follows.

5.1 *Varying System Parameter (VSP) Approach*

The VSP approach is based on a parametric generalization for various physical adjustments to the system's fundamental frequency, such as adding/removing the attached weights or lengthening/shortening the inertia arm. The indicated physical adjustments essentially result in a defining equation characterized by a targeted natural frequency. Hence, one can generalize these adjustments by directly examining the system parameters.

Substituting Eqn. (2) into Eqn. (1), removing the constant eccentric moment term and dividing the resulting equation by m gives

$$\ddot{\theta}(t)+2\zeta\omega_n\dot{\theta}(t)+\alpha_w\omega_n^2\theta(t)+(1-\alpha_w)\omega_n^2 z(\theta,\dot{\theta})=c_p a(t) \tag{6}$$

where

$$\zeta=\frac{c}{2\sqrt{mk}}, \qquad \omega_n=\sqrt{\frac{k}{m}}, \qquad \alpha_w=\frac{k_{p\delta}}{k},$$

$$k=k_{p\delta}+k_{ini}+k_l, \qquad c_p=\frac{c_f}{m}, \qquad z(\theta,\dot{\theta})=\frac{k_l\theta+h(\theta,\dot{\theta})}{k_l+k_{ini}} \tag{7}$$

Eqn. (6) is used to establish a_f on the condition that the CUF reaches unity at the end of the earthquake excitation. A frequency-independent damping ratio, ζ_s, is substituted for the analytical damping given by Eqn. (7). The value of ζ_s is the damping ratio resulting from the parameter identification procedure. Examining Eqn. (6), the free parameters controlling a_f involve only ω_n, c_p and the P-Δ stiffness ratio α_w.

The evaluation of a_c is essentially based on a linear response spectrum analysis of Eqn. (6) using a Code specified damping ratio ζ_c. Hence, the governing free parameters for a_c become ω_n and c_p only.

Replacing ω_n by R_w as the dependent parameter of a_c and a_f, the margin can be implicitly expressed as

$$M_r(R_w,\alpha_w,c_p)=\frac{a_f(R_w,\alpha_w,c_p)}{a_c(R_w,c_p)} \tag{8}$$

Although nonlinear analysis is performed in the fatigue analysis, the following amplification rules can be easily shown to be valid for an arbitrary constant λ.

$$a_c(R_w,\lambda c_p)=\frac{1}{\lambda}a_c(R_w,c_p) \qquad a_f(R_w,\alpha_w,\lambda c_p)=\frac{1}{\lambda}a_f(R_w,\alpha_w,c_p) \tag{9}$$

Substituting Eqn. (9) into Eqn. (8), the margin for a system with a participation factor λc_p is then derived as

$$M_r(R_w,\alpha_w,\lambda c_p)=M_r(R_w,\alpha_w,c_p) \tag{10}$$

Therefore, the seismic fatigue margin is independent of the value of λ and for any SDOF system expressible by Eqn. (6), the following parametric representation is valid

$$M_r = M_r(R_w, \alpha_w) \tag{11}$$

A margin spectrum based on this parametric representation is herein proposed. The margin is plotted as a function over a desired range of R_w using a fixed value of α_w. In addition, multiple margin curves representing different values of α_w can be simultaneously presented to account for the P-Δ effect.

5.2 *Varying Earthquake Time-Scale (VET) Approach*

The VET approach maintains the physical test system unaltered, but changes the predominant earthquake excitation frequency by compressing or stretching the input earthquake record in time. Let the earthquake time history be altered as $a(\lambda t)$. Then, the equation of motion using the VET approach can be expressed as

$$\ddot{\theta}(t) + 2\zeta\omega_n\dot{\theta}(t) + \alpha_w\omega_n^2\theta(t) + (1-\alpha_w)\omega_n^2 z(\theta,\dot{\theta}) = c_p a(\lambda t), \quad 0 \le t \le \frac{t_f}{\lambda} \tag{12}$$

where t_f is the total duration of $a(t)$ and other symbols are previously defined.

Consider the process of subdividing the response into a series of peak to peak response segments. The restoring force associated with each response segment represents a segment of the hysteresis curve between consecutive turning points. Denote each segment of restoring force as $\phi_i(\theta)$, which is a nonlinear function of θ only. Further, introduce a new time variable $\tau = \lambda t$ and denote differentiation with respect to τ by prime symbols. Then, each response segment as a function of τ is governed by

$$\theta''(\tau) + 2\zeta\frac{\omega_n}{\lambda}\theta'(\tau) + \alpha_w(\frac{\omega_n}{\lambda})^2\theta(\tau) + (1-\alpha_w)(\frac{\omega_n}{\lambda})^2\phi_i(\theta) = \frac{c_p}{\lambda^2}a(\tau) \tag{13}$$

This expression holds for hysteretic systems ranging from elasto-plastic type, bilinear type to the class of parallel-distributed-element systems being employed. One can sequentially concatenate each equation segment to form an entire response process as

$$\theta''(\tau) + 2\zeta\frac{\omega_n}{\lambda}\theta'(\tau) + \alpha_w(\frac{\omega_n}{\lambda})^2\theta(\tau) + (1-\alpha_w)(\frac{\omega_n}{\lambda})^2 z(\theta,\theta') = \frac{c_p}{\lambda^2}a(\tau), \quad 0 \le \tau \le t_f \tag{14}$$

The above expression is valid since $z(\theta,\theta')$ offers exactly the same sequence of restoring functions $\{\phi_0, \phi_1, \cdots, \phi_i, \cdots\}$ as that given by $z(\theta,\dot{\theta})$. This is because the nonlinear hysteresis term $h(\theta,\dot{\theta})$ depends on the sign but not the magnitude of velocity response.

Note that the presented transformation also holds for a linear consideration of Eqn. (12). In addition, both the strains in the fatigue failure model and the Code allowable maximum stress are independent of the time scale of the displacement time history. By treating the time variable as a dummy variable, the following system then possesses the same margin as that described by Eqn. (14).

$$\ddot{\theta}(t) + 2\zeta\frac{\omega_n}{\lambda}\dot{\theta}(t) + \alpha_w(\frac{\omega_n}{\lambda})^2\theta(t) + (1-\alpha_w)(\frac{\omega_n}{\lambda})^2 z(\theta,\dot{\theta}) = \frac{c_p}{\lambda^2}a(t), \quad 0 \le t \le t_f \tag{15}$$

Eqn. (15) is identical to the VSP approach in achieving a desired frequency ratio except for the denumerator λ^2 in the force participation term. Applying the fatigue margin's independence to the force participating factor as shown in Eqn. (10), it can be concluded that the margin is identically obtained by either the VET or VSP approach. However, the required

input intensity to achieve identical a_c and a_f levels for VET and VSP approaches will differ by a factor of λ^2 as stipulated in Eqn. (9).

6 STUDY RESULTS FOR TEST 36

Test 36 is a pressurized tee component test subjected to higher level PFDR input only in Run 7 and Run 8. This test was terminated half way into Run 8 due to a fatigue failure. The Run 8 data is used in PIPES to obtain an optimal nonlinear model. The measured and model simulated restoring moment-rotation hysteretic loops are compared in Fig. 3, and the rotation response time histories are compared in Fig. 4. The optimal model accurately reproduces the system response up to the time of failure when an abrupt change occurs in the measured data. The calibration of the fatigue damage based on a sequential range-pair counting method [3] and the ASME Code background document S-N curve [4] is illustrated in Fig. 5, where the CUF reaches unity at the time when the fatigue failure occurred.

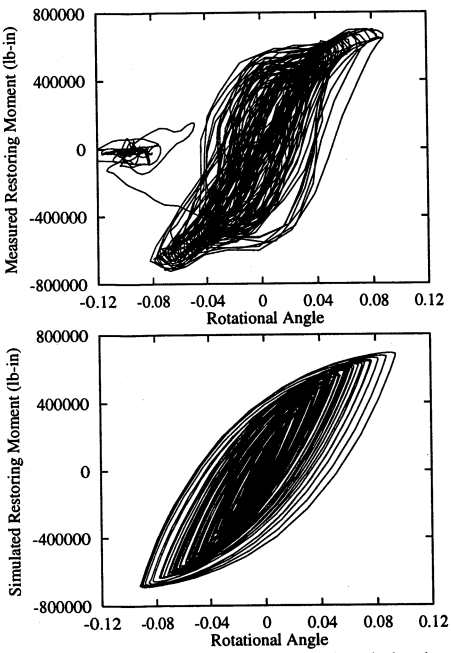

Figure 3: Comparison of measured and simulated hysteretic loops of Test 36, Run 8

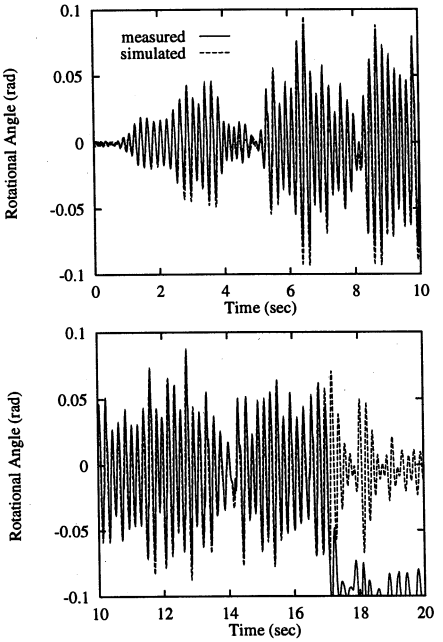

Figure 4: Comparison of measured and simulated response of Test 36, Run 8

This dynamic model and fatigue damage model are used with the VSP approach for varying R_w to generate the seismic fatigue margin spectra for the PFDR input loading. A fatigue margin factor, M_r / B_2, where B_2 is the Code primary stress index, is plotted for selected values of α_w in Fig. 6. It shows that the fatigue margin factors are relatively low for $R_w < 1$ with an increasing trend as R_w approaches 1, and remain above a level of 5 for $R_w > 1$. The effect of the P-Δ stiffness is shown to be insignificant to the fatigue margin factors. However, by plotting the CUF as a function of R_w and the peak input acceleration (Fig. 7), it shows the cliff-like profile introduced by the presence of P-Δ stiffness. This illustrates the

occurrence of dynamic instabilities caused by excessive rotational ratcheting for high R_w systems having higher degrees of P-Δ stiffness.

The higher fatigue margin factors at $R_w > 1$ and the likelihood of excessive rotational response for the aforementioned systems can also be demonstrated in Fig. 8, where three rotation time histories corresponding to R_w = 0.5, 1.5 and 3.0 with α_w= - 3 % are shown. These responses resulted from different levels of PFDR input loading but all possess the condition that CUF=1. It is observed that both the R_w = 1.5 and 3.0 response curves exhibit significant ratcheting behavior and result in large peak rotational angles.

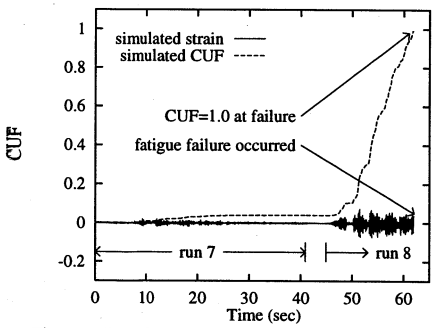

Figure 5: Simulated strain time history and evolutionary CUF for Test 36, β = 0.685, Sequential Method

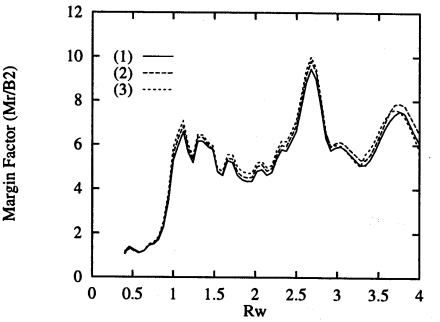

Figure 6: Margin spectra for Test 36 subjected to PFDR input, ζ_s =2 %, ζ_c = 5 %, (1): α_w = 5 %, (2): α_w = 0 %, (3):α_w = -5 %, Sequential Method

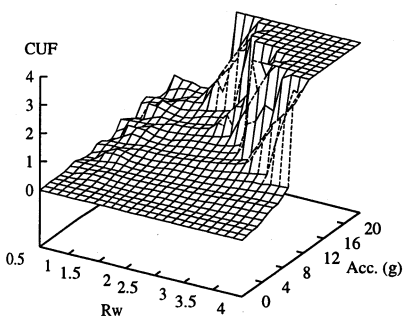

Figure 7: CUF as a function of R_w and peak acceleration of linearly amplified PFDR input for α_w = -5 %, c_p = 1 %, (profile is arbitrarily truncated at a level of CUF = 4)

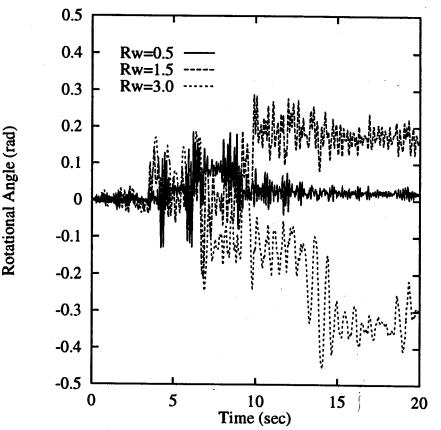

Figure 8: Response time history for various systems with CUF=1

To explain the larger rotational response at $R_w > 1$, one notices that for a SDOF system undergoing a fixed duration of excitation, the total number of response cycles decreases as the natural frequency decreases. Hence, larger average response ranges become necessary for a higher R_w system to achieve CUF=1, particularly at the low cycle end of linear logarithmic S-N plots where the fatigue usage fractions are relatively less sensitive to increases in strain amplitude.

The rotational ratchet behavior at $R_w > 1$ introduces strain accumulation that reduces fatigue life (fatigue-ratchet) and can result in instability or collapse failure before a through-wall crack forms. Such damage interaction and large deformation characteristics are not properly addressed by consideration of fatigue damage alone.

7 SUMMARY AND CONCLUSIONS

A framework for hysteretic modeling, model optimization and fatigue margin analyses for piping component seismic test systems was developed in this study. The developed models are capable of simulating the nonlinear response of the test systems with a high degree of accuracy. A unified treatment of frequency ratio effects on seismic fatigue margin is presented. The fatigue margin is concluded to be a two-parameter function of frequency ratio and P-Δ stiffness ratio. An exact proof is provided to show that the effect of R_w on fatigue margin can be identically obtained by varying the frequency of the physical model or varying the time scale of the input loading. The simulation results suggest the possibility of large-rotation induced damage mechanisms and failure modes that are not being addressed by a fatigue-based margin. The fatigue margin evaluation can be extended to include sustained weight moment effects and accumulated strain effects. The concept of a ductility-based margin against collapse is currently being considered by the authors to complement the use of the fatigue-based margin. Studies are also planned on material temperature effects on the fatigue and ductility margins.

DEDICATION

This paper is dedicated to the memory of Dr. W. P. Chen of ETEC, who was an original co-author of this paper. Dr. Chen skillfully managed the research described in this paper and made many significant technical contributions during the course of this study. His untimely death on January 4, 1997 represents an immense loss to the nuclear engineering community. He will be greatly missed by his colleagues.

ACKNOWLEDGMENTS

The authors are grateful to the NRC and ETEC for supporting the study reported in this paper. The views expressed in the paper are those of the authors and do not necessarily reflect the views or positions of the NRC or ETEC.

REFERENCES

1. Iwan, W. D. 1966, A Distributed-Element Model for Hysteresis and its Steady-State Dynamic Response, *Journal of Applied Mechanics*, 893.

2. Thyagarajan, R. S. 1989, *Modeling and Analysis of Hysteretic Structural Behavior*, Ph.D. Dissertation, California Institute of Technology, Pasadena.

3. Collins, J. A. 1981, *Failure of Materials in Mechanical Design*, Wiley-Interscience.

4. ASME, 1969. *Criteria of the ASME Boiler and Pressure Vessel Code for Design by Analysis in Section III and VIII,* Div. 2.